Evaluation of the GPM-IMERG Precipitation Product for Flood Modeling in a Semi-Arid Mountainous Basin in Morocco

Tarik Saouabe, El Mahdi El Khalki, Mohamed El Mehdi Saidi, Adam Najmi, Abdessamad Hadri, Said Rachidi, Mourad Jadoud, Yves Tramblay

water

MDPI

Article

Evaluation of the GPM-IMERG Precipitation Product for Flood Modeling in a Semi-Arid Mountainous Basin in Morocco

Tarik Saouabe [1], El Mahdi El Khalki [1], Mohamed El Mehdi Saidi [1], Adam Najmi [1], Abdessamad Hadri [1], Said Rachidi [2], Mourad Jadoud [3] and Yves Tramblay [4,*]

1 Georesources, Geoenvironment and Civil Engineering Laboratory, Cadi Ayyad University, Marrakech 40000, Morocco; saouabe.tarik@gmail.com (T.S.); Mahdi.khalki@gmail.com (E.M.E.K.); m.saidi@uca.ma (M.E.M.S.); adamnajmi12@gmail.com (A.N.); hadri.abdessamad@gmail.com (A.H.)
2 Tensift Hydraulic Basin Agency, Marrakech 40000, Morocco; rachidi.abht@gmail.com
3 Geosciences and Environmental Techniques Laboratory, Chouaïb Doukkali University, El Jadida 24000, Morocco; mourad_jadoud@yahoo.fr
4 HydroSciences Montpellier, University of Montpellier, CNRS, IRD, 34000 Montpellier, France
* Correspondence: yves.tramblay@ird.fr; Tel.: +33-4-67-14-33-59

Received: 4 August 2020; Accepted: 8 September 2020; Published: 9 September 2020

Abstract: A new precipitation dataset is provided since 2014 by the Global Precipitation Measurement (GPM) satellite constellation measurements combined in the Integrated Multi-satellite Retrievals for GPM (IMERG) algorithm. This recent GPM-IMERG dataset provides potentially useful precipitation data for regions with a low density of rain gauges. The main objective of this study is to evaluate the accuracy of the near real-time product (IMERG-E) compared to observed rainfall and its suitability for hydrological modeling over a mountainous watershed in Morocco, the Ghdat located upstream the city of Marrakech. Several statistical indices have been computed and a hydrological model has been driven with IMERG-E rainfall to estimate its suitability to simulate floods during the period from 2011 to 2018. The following results were obtained: (1) Compared to the rain gauge data, satellite precipitation data overestimates rainfall amounts with a relative bias of +35.61% (2) In terms of the precipitation detection capability, the IMERG-E performs better at reproducing the different precipitation statistics at the catchment scale, rather than at the pixel scale (3) The flood events can be simulated with the hydrological model using both the observed and the IMERG-E satellite precipitation data with a Nash–Sutcliffe efficiency coefficient of 0.58 and 0.71, respectively. The results of this study indicate that the GPM-IMERG-E precipitation estimates can be used for flood modeling in semi-arid regions such as Morocco and provide a valuable alternative to ground-based precipitation measurements.

Keywords: GPM; IMERG; precipitation; floods; Morocco; flood modeling

1. Introduction

The Mediterranean regions are often affected by deadly flood events that are considered as the most dangerous hydrometeorological risk [1]. Floods are essentially caused by intense precipitation [2,3] which can generate destructive floods that cause several deaths [4,5]. The Moroccan High Atlas is one of the most vulnerable areas to such extreme events [6]. There, in addition to the intense precipitation, steep slopes cause destructive floods [7], such as the catastrophic event of the Ourika valley in the summer of 1995 that caused several hundred deaths [8]. More recently, in autumn 2014, intense precipitation and major floods in southwestern Morocco caused 47 deaths [9,10] and in the summer of 2019 in the Anti-Atlas Mountain, a deadly flash flood caused seven deaths. Moreover, the random and

often unpredictable Wadi's flow in these areas requires careful study of their hydrological processes to control and better manage them.

To reduce the adverse effects of floods, several approaches are usually implemented. Some are structural, such as draining ditching [11] or building protective structures, such as dams [12]; other approaches rely on non-structural measures including hydrological modeling for flood forecasting, which has become a key tool for prevention but also to improve the alert systems design [13]. This modeling approach, benefiting from technological advances in computational tools, allows the analysis and simulation of the hydrological behaviors of streams [14–16]. Among these models, the rainfall-runoff models are often considered to simulate runoff [17]. They are based on a more or less detailed description of the basin's surface, topography, soil types, and land use. These variables can be explicitly included in the model or not, depending on the data availability.

The physically-based hydrological models require several physical measurements distributed over a catchment, which often requires costly monitoring strategies, and in the case of Morocco this type of data is rarely available [7,18]. Oppositely, conceptual or empirical models only require a long time series of observed data to obtain a robust model evaluation allowing for their use to issue forecasts, so they are usually preferred for operational and real time applications [19]. In Morocco, the long time series is often available only at the daily time step. However, the time of the concentration of floods can be only a few hours in most Mediterranean basins in the case of fast floods, a type of flood prominent in semi-arid regions such as Morocco. Therefore, the application of hydrological modeling is challenged with the lack of the meteorological data at a fine temporal resolution, as is the case in the majority of North African countries. To deal with this problem, satellite precipitation products could be extremely useful, particularly in ungauged catchments or in areas with a low density of hydrometeorological monitoring networks [20–22] or even over the land areas where the spatial coverage from surface observations is not uniform [23].

In recent years, rainfall products derived from satellites have been developed and released to the scientific community. Among these products, the Precipitation Estimation from Remotely Sensed Information using Artificial Neural Networks (PERSIANN) [24], the National Oceanic and Atmospheric Administration Climate Prediction Center morphing technique product (CMORPH) [25], the Tropical Rainfall Measuring Mission (TRMM) Multi-satellite Precipitation Analysis products (TMPA) [26] and the Global Precipitation Measurement (GPM) [27] have been released. Several inter-comparison studies have been performed to evaluate the validity of precipitation satellite estimates in many fields, such as for hydrological simulation and water resources management at different spatial and temporal scales [28–36].

As the successor of TRMM, the GPM mission has been launched in 2014 by the National Aeronautics and Space Administration (NASA) and the Japanese Aerospace Exploration Agency (JAXA). Compared to TRMM, GPM incorporates three important improvements: (1) greater coverage of climate zones because of the increase in the orbital inclination angle of the GPM satellite from 35° in the TRMM satellite to 65°, (2) liquid and solid precipitation detection based on "high-frequency" passive microwave channels (165.5 and 183.3 GHz) (3) greater sensitivity of dual-frequency precipitation radar (DPR) to light precipitation and snowfall [26,37,38]. The GPM products are divided into different categories, the early, late, and final runs corresponding to IMERG-E, IMERG-L and IMERG-F, respectively. These products have a high spatial ($0.1° \times 0.1°$) and temporal (30 min) resolution within the 60° N–S latitude band, that could provide precipitation at the adequate spatio-temporal resolutions for flood monitoring.

In Morocco, some studies have evaluated the performance of TRMM products. For instance, ref. [39] evaluated four TMPA products (3B42: V6, V7temp, V7, RTV7) against 125 rain gauges depending on climatic zones and topography in Northern Morocco for the period 1998–2012. They concluded that the TMPA research products (3B42 V6 and V7) performed better than the real-time product (3B42 RT). Further, ref. [22] assessed five different satellite-based precipitation products (TRMM-3B42 v6 and v7, RFE 2.0, PERSIANN-CDR, CMORPH1.0 version 0.x) in north Morocco. They indicated that the TRMM-3B42 v7 product is the closest to rain gauges data and can be used for

hydrological modeling. Ref. [40] evaluated The TRMM 3B42 Version 7 product by using rain gauges measurements from 19 stations in the Oum-ErBia basin from 1998 to 2011. They indicated that this satellite product provides poor estimations of rainfall at the daily time scale but improved accuracy at monthly and annual time scale.

No studies have been conducted so far to evaluate the GPM–IMERG product for flood modeling, neither in Morocco nor in Maghreb countries with similar climatic conditions. To fill this gap, the purpose of this study is to evaluate (i) the accuracy and performance of the GPM–IMERG product to reproduce observed rainfall and (ii) the capability to model flood events with a hydrological model based on Soil Conservation Service-Curve Number (SCS-CN). This type of model is chosen since it is widely used in the Mediterranean region for floods [3]. This model could serve as a tool to assist decision makers (water basin agencies, water departments) in flood prediction and management, as traditional warning systems do not provide forecasts in time for effective intervention [41].

2. Study Area and Data

2.1. Study Area and Hydro-Rainfall Data

The Ghdat watershed is located in the upstream of the large Tensift basin which drains the High Atlas of Marrakech (Figure 1). Covering an area of 552 km^2, the altitudes are ranging from 693 to 3578 m. The basin, whose average altitude is 1730 m, has a large zone located between 1000 and 2600 m representing 82% of the basin's area. The average slope over the catchment, measured from a 30 m digital terrain model, is 30.7%.

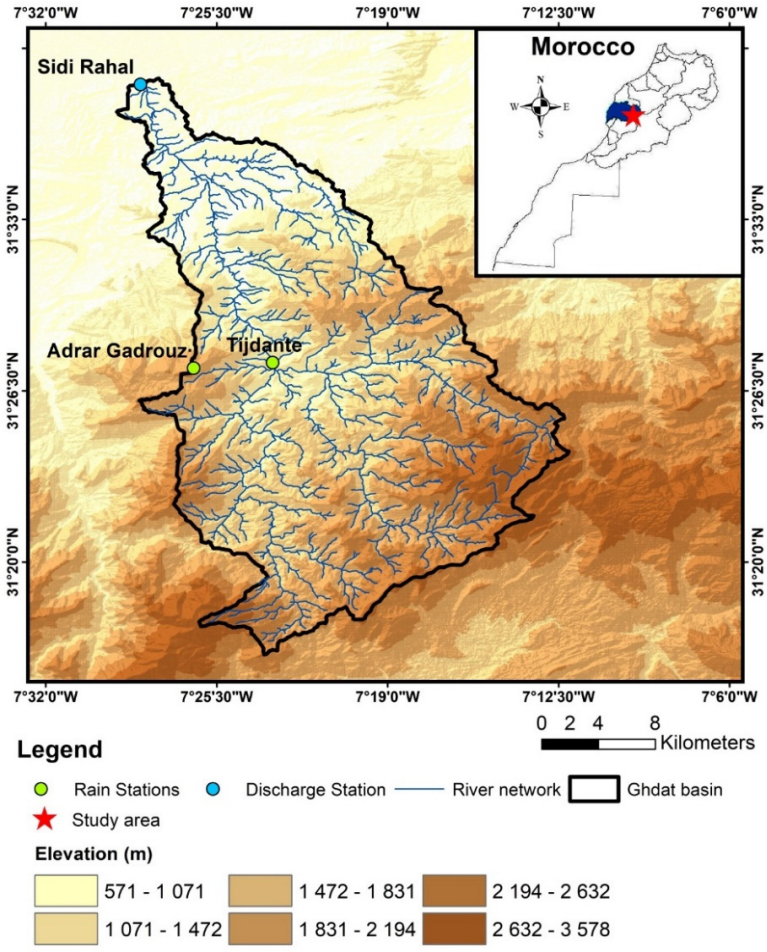

Figure 1. Geographical location of the Ghdat watershed and hydro-rainfall stations.

Geologically, the basin consists of two large groups: on the one hand, a rigid Paleozoic and Pre-Cambrian basement upstream, dominated by schists and quartzites, and downstream, soft Permo-Triassic deposits including sandstones, clays, conglomerates and marl-limestones of the Cenozoic age [42–44]. These formations are generally semi-permeable and favor heavy runoff in the case of intense rain. The hydrometric station of Sidi Rahal located at an altitude of 690 m, controls the discharge of the Ghdat Wadi and also serves as a rain gauge. It receives an average of 359 mm of rainfall per year. Rainfall and discharge data cover a 50-year period from the 1967–1968 to 2016–2017 hydrological years. These data come from gauges installed by the Tensift Hydraulic Basin Agency in Marrakech. This agency installed two other rain gauges upstream of the basin: Adrar Gardouz and Tijdante at altitudes of 2285 m and 1122 m, respectively. This made the Ghdat basin instrumented by three rainfall gauges (Sidi Rahal, Adrar Gardouz and Tijdante) and a hydrometric station (Sidi Rahal) (Table 1).

Table 1. Situation and period of measurement of hydro-rainfall stations.

Station	Type	Longitude	Latitude	Altitude (m)
Sidi Rahal	Rain and river discharge	−7.47	31.64	687
Adrar Gardouz	Rain	−7.44	31.46	2285
Tijdante	Rain	−7.39	31.46	1122

The time step of the rainfall and runoff data is 10 min. The data for modeling covers a period from 2011 to 2018. A total of 17 flood events are selected from the hydro-meteorological data. The observed precipitation data at 10-min time step were converted to 30-min to be compared with the satellite data.

2.2. The GPM IMERG-E Satellite Precipitation Product

The GPM mission, as an advanced successor to the TRMM, provides new global rainfall and snowfall observation products. The GPM Core Observatory satellite was launched in February 2014 by NASA and JAXA, equipped with a Dual-frequency Precipitation Radar (DPR) and a GPM Microwave Imager (GMI). The GPM mission has different products, organized using three levels: Level-1 (IMERG-E), Level-2 (IMERG-L), and Level-3 (IMERG-F). The IMERG system is run in near-real time and provides IMERG-E and IMERG-L with 4-h and 12-h latencies, respectively. The IMERG-F is calibrated with rain gauge analyses by the Global Precipitation Climatology Center (GPCC) and then would be available after 3.5 months. These products are provided at 0.1° × 0.1° spatial scale between 60° S–60° N and at half-hourly time scale. In this study, IMERG-E half-hourly data from 2011 to 2018 were downloaded from the NASA website (https://gpm.nasa.gov/data-access/downloads/gpm). This product was chosen due to its short time latency (4-h), making it interesting for the early warning of flood events. We extracted four pixels of GPM IMERG-E that cover the Ghdat basin and we interpolated observed precipitation data with the inverse distance method to represent areal precipitation over the studied basin.

2.3. Soil Moisture Dataset

To estimate the initial soil moisture condition prior to flood events, the European Space Agency Climate Change Initiative (ESA-CCI) data is considered. ESA-CCI V04.2 is a soil moisture product (http://www.esa-soilmoisture-cci.org/) available over a 38-year period from 1978 to 2018. This database includes three products: active, passive and combined. It provides daily soil surface moisture with a spatial resolution of 0.25 degrees [31,45,46]. The product has been validated by [47], and recently validated in the High Atlas of Marrakech by [18,48] for flood modeling. The ESA-CCI product shows in the mountainous area some missing values [49] that are related to a filter that is applied to the ESA-CCI product in order to ensure the data quality [45]. The ESA-CCI soil moisture pixel covering the Ghdat basin has been extracted.

3. Methods

In this section we describe the methodology adopted for the statistical and hydrological evaluation of GPM IMERG-E at different time scale. First, we compare the GPM IMERG-E product extracted from January 2011 to December 2018, against the ground precipitation observations using statistical indices. Second, hydrological simulations of flood events using a hydrological model is performed with either rain gauge data or GPM IMERG-E precipitation data.

3.1. Statistical Evaluation of Satellite Precipitation Products

To evaluate the accuracy of the GPM IMERG-E product against rain gauge observations in both at basin and grid-cell scale that corresponds to the GPM pixel covering the rain gauge. Four statistical indices were adopted; The Pearson's correlation coefficient (CC) describes the agreement between the satellite precipitation and ground observations (Equation (1)). Mean error (ME) measures the average error magnitude of satellite precipitation (Equation (3)). Root-mean square error (RMSE) indicates the average error magnitude between satellite data and observed precipitation data (Equation (4)). Relative bias (BIAS) reflects the systematic bias between the SPPs and the ground observations (Equation (2)). These indices are expressed as follows:

$$C = \frac{\sum_{i=1}^{n}(G_i - \overline{G})\left(S_i - \overline{S}\right)}{\sqrt{\sum_{i=1}^{n}(G_i - \overline{G})^2} \times \sqrt{\sum_{i=1}^{n}(S_i - \overline{S})^2}} \quad (1)$$

$$Bias = \frac{\sum_{i=1}^{n}(S_i - G_i)}{\sum_{i=1}^{n} G_i} \times 100 \quad (2)$$

$$ME = \frac{\sum_{i=1}^{n}(S_i - G_i)}{n} \quad (3)$$

$$RMSE = \sqrt{\frac{\sum_{i=1}^{n}(S_i - G_i)^2}{n}} \quad (4)$$

where n is the sample size; S_i is the satellite precipitation estimate; G_i is the gauge observation; S is the mean satellite precipitation estimate; G is the mean gauge observation.

Moreover, to quantitatively evaluate the precipitation detection ability of the satellite precipitation against the rain gauge observations, we used two indices that are based on the contingency table of satellite precipitation estimates with observations. The probability of detection (POD) (Equation (5)) measures the fraction of precipitation events correctly detected by the satellite. The false alarm ratio (FAR) (Equation (6)) describes the fraction of false events detected by the satellite. (Table 2).

Table 2. The contingency table used to estimate the precipitation detection ability of the satellite precipitation. POD: probability of detection, FAR: false alarm ratio.

		Observation		
		Yes	**No**	
GPM IMERG-E	**Yes**	A: Hits	B: False	A + B: Observed by satellites
	No	C: Misses	D: Rejection	C + D: Not observed by satellites
		A + C; Observed by rain gauges	B + D: Not observed by rain gauges	N: Total of events

$$POD = A/(A + C) \quad (5)$$

$$FAR = B/(A+B) \tag{6}$$

3.2. Hydrological Model

In this study, we used the SCS-CN model implemented in the HEC-HMS software [50]. This software includes hydrological analysis procedures such as unit hydrographs and hydrologic routing (http://www.hec.usace.army.mil/software/hec-hms/). The SCS-CN model is based on the cumulative excess of precipitation by time [50]:

$$Pe = (P - 0.2S)2/P + 0.8S \tag{7}$$

where Pe is the excess of precipitation at time t, P is the rain accumulation at time t and S is the maximum retention capacity, that is related to the curve number (CN).

The excess precipitation is transformed into direct runoff through the concept of unit hydrograph. The modeling tool used has several transfer functions: Clark, Snyder and SCS unit hydrographs, Modclark transformation and the kinematic wave. For event modeling, Clark's unit hydrograph [50] has been widely used in the semi-arid mountainous basins which are known by a complex and variable topography [18,51]:

$$\frac{A_t}{A} = \begin{cases} 1.414\left(\frac{t}{t_c}\right)^{1.5} & for\ t \le \frac{t_c}{2} \\ 1 - 1.414\left(1 - \frac{t}{t_c}\right)^{1.5} & for\ t \ge \frac{t_c}{2} \end{cases} \tag{8}$$

where A_t is the area of the watershed, contributing at time t, A is the total watershed area, t_c is the time of concentration of the watershed.

3.3. Hydrological Model Calibration and Validation

The calibration process aims to find the optimal parameters to minimize the objective function. The calibration for each parameter is performed independently of the others, to avoid interdependence between the parameters of the production and transfer functions. The calibration is performed both automatically and manually, to assess the sensitivity of the model to small variations of the parameters. Three efficiency criterions were used to evaluate the agreement between observed and simulated hydrographs; The Nash Sutcliffe (NS) efficiency coefficient [52] (Equation (9)) and the relative error calculated based on the observed and estimated total volume runoff and peak flow (bias) (Equations (10) and (11))

$$NS = 1 - \frac{\sum_{i=1}^{n}(Q_{o,i} - Q_{s,i})^2}{\sum_{i=1}^{n}\left(Q_{o,i} - \overline{Q_o}\right)^2} \tag{9}$$

$$BIAS_V = \frac{(V_s - V_o)}{V_o} \tag{10}$$

$$BIAS_Q = \frac{(Q_s - Q_o)}{Q_o} \tag{11}$$

where $Q_{o,i}$ and $Q_{s,i}$ are the observed and the simulated flow, respectively, and $\overline{Q_o}$ is the average observed flow. V_s and V_o are the simulated and the observed runoff depth, respectively.

The CN parameter can be identified as the initial soil moisture condition in the model. Several studies have shown that this parameter can be related to different soil moisture indicators, obtained from field measurements [53–55], or soil moisture models or from satellite data [56] to reproduce the CN of flood events. In the present study, the approach previously used by [18,48] in a similar basin of South Morocco is implemented: the ESA-CCI soil moisture is used to estimate the initial soil moisture condition. All the model parameters including the CN are first calibrated. Then a linear regression is established between the CN and the ESA-CCI soil moisture the day before of each flood event.

For validation, a leave-one-out procedure (or Jack Knife) is considered, with each flood event in turn removed from the sample, the model is recalibrated on the remaining events. The mean values of the model parameters obtained after recalibration are used for the validation of the event that was removed. For the CN, the value is estimated from the linear regression against ESA-CCI soil moisture.

4. Results

4.1. GPM IMERG-E Product Evaluation

The GPM IMERG-E product is evaluated against the rain gauge data using six statistical indices considered (CC, ME, RMSE, BIAS, POD and FAR) at both basin scale and the individual grid-cells corresponding to rain gauges during the available period from January 2011 to December 2018. The statistical evaluation indices of the IMERG-E product are presented at the basin scale in Table 3 and at the grid-cell scale in Table 4.

Table 3. Evaluation indices of IMERG-E at basin scale for the entire period (2011–2018).

Time Scale	CC	ME (mm)	RMSE (mm)	BIAS (%)	POD	FAR
Hourly	0.10	0.02	0.84	35.61	0.36	0.86
Daily	0.14	0.44	9.88		0.68	0.63

Table 4. Evaluation indices of IMERG-E at the grid-cell scale for the entire period (2011–2018).

Pixel	Time Scale	CC	ME (mm)	RMSE (mm)	BIAS (%)	POD	FAR
GPM-Adrar	Hourly	0.03	0.00	2.05	95.67	0.24	0.91
	Daily	0.08	0.07	24.15		0.57	0.72
GPM-Sidi Rahal	Hourly	0.26	0.03	0.61	3.99	0.25	0.90
	Daily	0.37	0.63	5.73		0.47	0.76
GPM-Tijdante	Hourly	0.00	0.02	0.84	143.29	0.11	0.97
	Daily	−0.02	0.51	9.32		0.40	0.83

At the basin scale, satellite precipitation data overestimates the amount of rainfall with a relative Bias of +35.61%. Several studies found that the IMERG precipitation products overestimate the amount of rainfall; in Italy [57], in Peru and Ecuador [58], in Iran [59] and in Spain [60].

About the overall agreement between the gauge observations and satellite precipitation data, the Pearson's correlation coefficient is equal to 0.10 and 0.14 at the hourly and daily time scale, respectively. Therefore, the accuracy of IMERG-E data improved over the daily time scale.

In terms of precipitation detection capability, the near real time IMERG-E precipitation data presents satisfactory performance and can be used to detect rain events over the Ghdat basin. The same results have been found in Spain with a low bias in the IMERG-E product that allows near-real time applications [61]. The daily estimates had a higher POD equal to 0.68 and a smaller FAR equal to 0.63 compared to the hourly (POD = 0.36 and FAR = 0.86) time scale.

For the grid-cell evaluation, the comparison of IMERG-E data with the data at the Sidi Rahal rain-gauge presents higher performance compared with others pixels; in which the RMSE is lower at the hourly time scale. Concerning the agreement between observed and satellite precipitation data, Sidi Rahal also shows the higher correlation coefficients compared to the other gauges. The GPM IMERG-E presents slightly higher performance in the downstream part of the studied basin. These results may be reflected the impact of the complex topography in the upstream portions of the basin. The good agreement between observed and satellite precipitation at the Adrar station is probably due to the very good quality of the data at this station; this gauge is located at a relatively high altitude but in an open area where there is no relief effect affecting rain measurements. This gauge is also

considered by the Tensift Hydraulic Basin Agency as reference station, that is also used to relay data transmission from the other gauges with a poorer network coverage.

Several studies presented similar or comparable results. In terms of elevation effects on the IMERG product performance, in the Ebro River basin in Spain the IMERG performance strongly depends on elevation [60]. Additionally, in the arid western China with high altitudes, the performance of IMERG is less satisfactory than in south and east China, indicating a significant impact of topography [62]. Moreover, the IMERG presented better performance at low latitudes than at middle latitudes over mainland China [37]. Overall, the results of this statistical evaluation indicated that the IMERG-E achieved a better performance at the basin scale at hourly and daily time scales rather than at the pixel scale.

4.2. Hydrological Model Calibration

For rain gauge-based precipitation data, The NS values range from 0.40 to 0.97 with an average of 0.77. The calibrated model parameters are shown in Table 5. The mean relative bias on peak discharge and volume for all events are −7.07% and −0.7%, respectively (Table 6). For the events simulated with the GPM IMERG-E product, the average of NS is equal to 0.74 with a relative bias on peak discharge and volume of −20.57% and 3.99%, respectively. Thus, it can be concluded that the 17 events are well simulated (Figure 2). The model was able to reproduce the peak discharge and the shape of different hydrographs for the events occurred in the studied basin between 2011 and 2018 for both rain gauge-based precipitation data and satellite precipitation data (Figure 2 and Figure 4). These results are similar to the study of [63], who found that IMERG-E gave a good performance in term of model calibration using the HEC-HMS model. The overestimation of flood volume with GPM IMERG-E is consistent with the positive bias in IMERG-E found in the previous section. Table 5 shows the calibrated model parameters with observed or IMERG-E precipitation data. The CN values are very similar between the simulations with observed or IMERG-E precipitation. For some events, the Tc and Sc parameters show a greater variation between the two different sources of precipitation data, mostly due to compensation effects during calibration due to different rainfall inputs.

Table 5. Calibrated parameters of the hydrological model.

Event	CN		Time of Concentration		Storage Coefficient	
	Observed	GPM	Observed	GPM	Observed	GPM
01/05/2011	93.4	98.1	5.5	2.5	1.4	1.2
02/05/2011	94.3	97.1	4.3	7.5	0.7	5.0
29/03/2012	88.3	88.0	4.8	6.5	4.8	5.0
01/12/2012	86.7	86.0	1.2	1.5	5.8	4.4
17/09/2013	86.1	90.0	0.2	0.9	0.4	0.1
21/09/2014	86.9	84.0	1.8	9.3	1.5	1.7
05/11/2014	63.8	60.0	9.5	8.2	2.5	12.9
09/11/2014	80.1	81.0	0.1	4.5	2.0	0.8
22/11/2014	84.5	83.0	0.1	0.0	15.0	3.2
28/11/2014	90.2	90.0	0.1	4.5	5.0	1.0
19/01/2015	77.8	72.0	2.6	9.0	1.8	2.0
22/03/2016	98.9	99.0	5.8	9.0	3.0	2.0
27/11/2016	96.3	98.0	5.4	1.0	2.0	1.7
16/12/2016	82.7	80.0	0.1	6.0	1.2	1.0
23/04/2018	71.7	70.0	2.0	1.6	0.7	0.1
25/04/2018	86.7	85.0	5.7	5.1	0.5	2.2
31/10/2018	77.8	76.0	0.1	8.0	2.1	2.0

Table 6. Calibration and validation results.

Events	Calibration						Validation					
	Nash		BiasQ (%)		BiasV (%)		Nash		BiasQ (%)		BiasV (%)	
	Observed	GPM	Observed	GPM	Observed	GPM	Observed	GPM	Observed	GPM	Observed	GPM
01/05/2011	0.7	0.9	−31.3	0.0	2.7	2.9	0.4	N.A.	−49.0	−84.9	−27.0	−27.0
02/05/2011	1.0	0.7	0.0	−11.6	1.0	11.4	0.2	N.A.	−50.0	−71.6	−30.8	−30.8
29/03/2012	0.7	0.7	−4.8	−28.6	−11.0	−3.2	0.6	0.7	13.2	−28.2	4.5	−1.9
01/12/2012	0.9	0.9	0.0	−0.9	−0.4	−1.1	0.9	0.9	−0.3	−0.3	−0.4	−0.7
17/09/2013	0.9	0.7	−1.3	−15.3	0.0	22.2	N.A.	0.7	547.4	−12.2	445.4	22.2
21/09/2014	0.7	0.7	1.0	−19.6	0.0	−4.7	N.A.	0.7	−46.8	−13.0	−35.7	2.3
05/11/2014	0.9	0.8	−9.9	−4.0	−2.2	−2.2	0.9	0.8	−9.9	−6.1	−2.2	−4.3
09/11/2014	0.6	0.9	10.1	−7.2	0.8	3.1	N.A.	0.8	86.7	−3.4	54.1	5.4
22/11/2014	0.4	0.4	−5.7	−94.7	24.4	1.1	0.3	0.4	−1.4	−23.2	30.1	4.9
28/11/2014	0.4	0.8	6.6	−8.9	32.7	14.3	0.5	0.8	1.0	−5.0	25.1	21.1
19/01/2015	1.0	0.9	−4.5	−16.3	−2.3	2.3	0.9	0.8	−16.7	−10.1	−7.8	6.1
22/03/2016	1.0	0.7	−8.6	−23.8	−2.1	2.1	0.9	0.7	1.0	−23.8	6.3	2.1
27/11/2016	0.9	0.7	−3.7	−17.1	−4.3	−8.6	N.A.	0.6	−78.3	−17.1	−71.2	−16.1
16/12/2016	0.7	0.6	2.9	−35.3	−11.2	10.0	0.4	0.6	−40.2	−36.4	−47.2	16.7
23/04/2018	0.6	0.7	−40.0	−14.0	−38.3	8.1	0.6	0.7	−40.0	−14.0	8.1	−2.7
25/04/2018	0.9	0.7	−24.1	−31.9	−0.9	6.0	0.6	0.7	−50.3	−31.9	−27.2	5.1
31/10/2018	0.8	0.9	−3.2	−24.7	0.7	1.8	0.4	0.9	19.6	−31.0	22.5	−6.0
Mean	0.8	0.7	−6.8	−20.8	−0.6	3.9	0.6	0.7	16.8	−24.2	20.4	−0.2

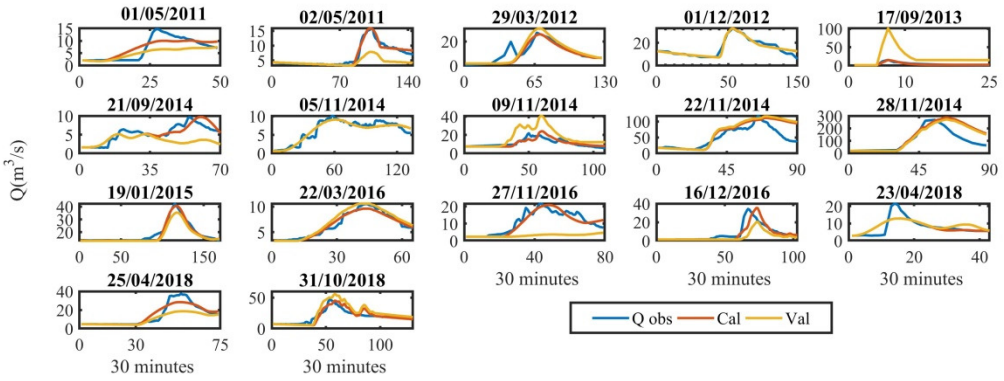

Figure 2. Floods simulated with observed precipitation.

Despite the fact that IMERG-E better reproduces observed rainfall at the daily time step rather than at the hourly time step, the hydrological model driven by IMERG-E is able to reproduce floods with a good efficiency. This could be partly explained by the fact that the hydrological model parameters are being calibrated, so the adjustment of its parameters makes it possible to compensate for the bias on the satellite precipitation. This can be seen in the Sc and Tc parameter values (Table 5) that are quite different between observed precipitation and IMERG. We also note slightly higher average CN values with the observed than with the IMERG precipitation, due to the overestimation of IMERG compared to the observed rainfall.

4.3. Hydrological Model Validation with Observed and GPM IMERG-E Precipitation

The calibrated CN are correlated with the ESA-CCI soil moisture data in order to estimate the initial soil moisture condition of the model. This correlation is good with a coefficient equal to r = 0.96 when the SCS-CN model is calibrated with rain gauge data (Figure 3).

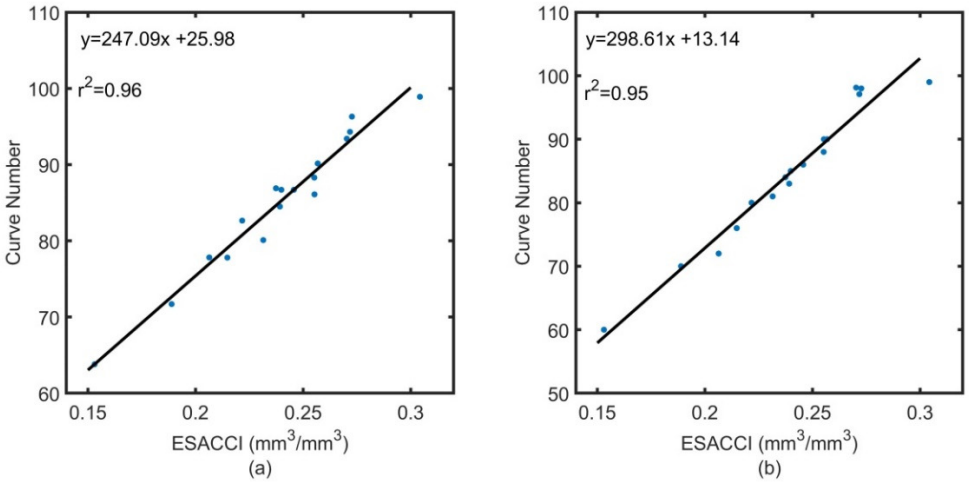

Figure 3. CN correlation with soil moisture data for observed (**a**) and Global Precipitation Measurement (GPM) events (**b**).

For the data based on the IMERG-E satellite precipitation, the correlation between the CN and the ESA-CCI data are also strong and equal to 0.95 (Figure 3). This correlation confirms the good relationship between the CN parameter of the production function and ancillary source of soil moisture conditions, as demonstrated in similar studies [18,55,64]. The validation will therefore be based on ESA-CCI data.

The equation based on the correlation allowed us to calculate the validation CN of each event in turn by the leave-one-out method. This method involves correlating the calibrated CN values of the sixteen events with ESA-CCI soil moisture to determine the CN of the event that remains.

Table 6 presents the results of the efficiency criterions used to evaluate the agreement between observed and simulated hydrographs. For the validated events, the average Nash values is equal to 0.58. The mean relative bias on peak discharge and volume are 16.8% and 20.4%, respectively. Concerning the events modeled with satellite rainfall, the model presents slightly better performances with a NS raised to 0.71. The relative bias on peak discharge and volume are −24.2% and −0.2%, respectively.

We were able to validate 13 out of 17 events simulated with rain gauge data (Figure 2) and 15 events for satellite precipitation data (Figure 4). It should be noted that this validation experiment combines the uncertainties stemming from the CN/ESA-CCI soil moisture relationship but also the uncertainties on precipitation estimates of the IMERG-E product. For non-validated events from observed data (i.e., with very low negative Nash values reported as N.A. in Table 6), a detailed analysis of the results reveals that for these events, the difference in CN values between calibration and validation is three time larger than the difference in CN values for the other events. Therefore, this indicates that for some events a slight change in the CN values can have a strong negative impact on the results. This finding denotes the importance of the soil moisture data to adequately estimate the antecedent soil moisture conditions, for the validation of flood events in a semi-arid environment [18,51,65].

For the floods simulated with satellite precipitation data, the events of the 1 May 2011 and 2 May 2011 present higher values of CNs in calibration compared to other events. For these two events, the cumulative rainfall recorded which is very low (2.36 mm and 4.44 mm, respectively) and the high CN values obtained reflect the overestimation of rainfall by IMERG-E. It would be required then for these two events to increase the value of the CN in order to adequately reproduce the observed hydrograph. It should be noted also that events modelled with ground observation or satellite precipitation do not have the same performances in terms of Nash, relative bias on flow and volume. We also compared the spatial variability of rainfall fields for each event, but there is no apparent link between the hydrological model performance to reproduce floods and the spatial variability of rainfall during the event.

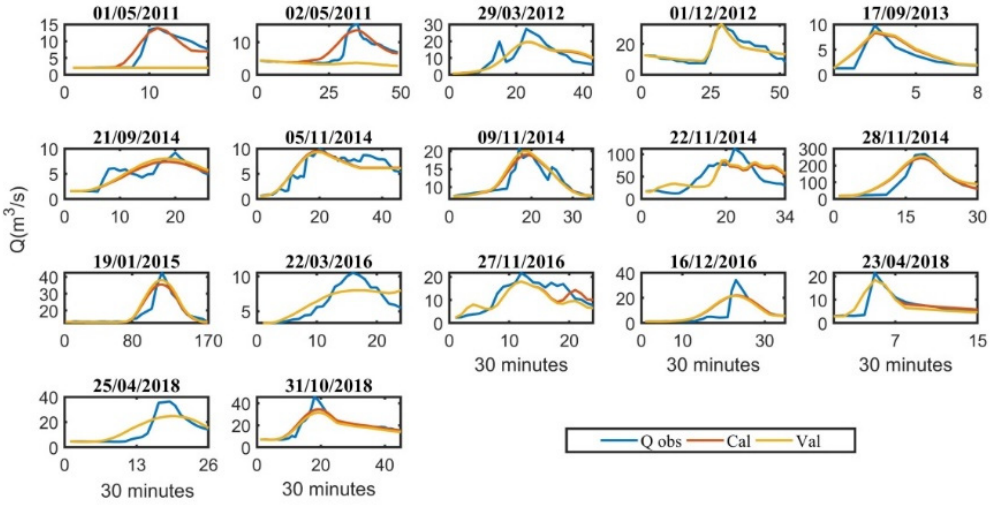

Figure 4. Floods simulated with GPM IMERG-E precipitation.

5. Conclusions

This study conducted a first assessment of the near real-time satellite precipitation product GPM IMERG-E in Morocco for flood modelling. In this work, an event-based hydrological model was developed for a semi-arid mountainous watershed based on two sources of precipitation (observed and estimated from IMERG-E). Following the determination of model parameters, calibration and validation tests, the model was able to reproduce flood hydrographs at a short time step, which is adapted to this type of semi-arid small basin. The main findings of this study are summarized as follows:

(1) Compared to the rain gauge data, satellite precipitation data overestimates the amount of rainfall with a relative Bias of 35.61%.
(2) At the hourly and daily time scales, the GPM IMERG-E presents a fair accuracy to reproduce precipitation amounts and detect precipitation occurrence, with better performances at the daily time step.
(3) The comparison reveals that basin-averaged GPM IMERG-E precipitation is in better agreement with interpolated precipitation over the catchment from observed data than a direct pixel-to-station comparison.
(4) The flood events can be simulated using either satellite or rain-gauge precipitation with NS criterions of 0.58 and 0.71, respectively.

To conclude, the studied satellite precipitation product presents satisfactory performance in terms of statistical evaluation and hydrological modeling. For hydrological purposes, this source of precipitation could be used in ungauged basins and in data scarce regions like Morocco for flood modelling and contribute to the development of early warning systems. Concerning the application of the IMERG product in hydrological modeling, ref. [66] previously noted that the product was suitable for heavy precipitation and [61] showed the potential added value of the IMERG-E product in near-real time applications.

There is a need for further evaluation studies of this satellite product for hydrological modeling in other basins in north Africa and other semi-arid regions with similar climate characteristics. The type of event-based models developed in the present study with satellite precipitation and soil moisture data would represent an interesting alternative to continuous models since the data requirements for this type of approach are limited and could rely on remote sensing products, with GPM IMERG-E data for precipitation and ESA-CCI soil moisture. This model could be applied to simulate floods in un-gauged basins or basins where only daily data for precipitation and river discharge are available. This modelling scheme could be a valuable tool to help decision-makers (watershed agencies, water

services) and to understand the watershed behavior during heavy rainfall episodes and better manage flood risks. To this end, the development of early warning systems for flood alerts would provide viable opportunities to reduce the damage to properties and fatalities linked to floods.

Author Contributions: Conceptualization, T.S. and E.M.E.K.; methodology, T.S., E.M.E.K., M.E.M.S., A.N., A.H., Y.T.; writing—original draft preparation, T.S., E.M.E.K., M.E.M.S.; writing—review and editing, T.S., E.M.E.K., M.E.M.S., A.N., A.H., S.R., M.J., Y.T. All authors have read and agreed to the published version of the manuscript.

Funding: This research received no external funding.

Acknowledgments: The authors would like to express their gratitude for the Agence de Bassin Hydraulique du Tensift for providing the data required for this study.

Conflicts of Interest: The authors declare no conflict of interest.

References

1. Llasat, M.C.; Llasat-Botija, M.; Prat, M.A.; PorcúPorc, F.; Price, C.; Mugnai, A.; Lagouvardos, K.; Kotroni, V.; Katsanos, D.; Michaelides, S.; et al. High-impact floods and flash floods in Mediterranean countries: The FLASH preliminary database. *Adv. Geosci.* **2010**, *23*, 47–55. [CrossRef]
2. Gao, X.; Pal, J.S.; Giorgi, F. Projected changes in mean and extreme precipitation over the Mediterranean region from a high resolution double nested RCM simulation. *Geophys. Res. Lett.* **2006**, *33*. [CrossRef]
3. Merheb, M.; Moussa, R.; Abdallah, C.; Colin, F.; Perrin, C.; Baghdadi, N. Hydrological response characteristics of Mediterranean catchments at different time scales: A meta-analysis. *Hydrol. Sci. J.* **2016**, *61*, 2520–2539. [CrossRef]
4. Douglas, I.; Alam, K.; Maghenda, M.; Mcdonnell, Y.; Mclean, L.; Campbell, J. Unjust waters: Climate change, fl ooding and the urban poor in Africa. *Environ. Urban.* **2008**, *20*, 187–205. [CrossRef]
5. Di Baldassarre, G.; Montanari, A.; Lins, H.; Koutsoyiannis, D.; Brandimarte, L.; Blschl, G. Flood fatalities in Africa: From diagnosis to mitigation. *Geophys. Res. Lett.* **2010**, *37*. [CrossRef]
6. Saidi, M.; Daoudi, L.; Aresmouk, M.; Blali, A. Rôle du milieu physique dans l'amplification des crues en milieu montagnard: Exemple de la crue du 17 août 1995 dans la vallée de l'Ourika (Haut-Atlas, Maroc). *Rev. Sécheresse Paris* **2003**, *14*, 107–114.
7. Chaponnière, A.; Boulet, G.; Chehbouni, A.; Aresmouk, M. Understanding hydrological processes with scarce data in a mountain environment. *Hydrol. Process. Int. J.* **2008**, *22*, 1908–1921. [CrossRef]
8. Vinet, F.; El Mehdi Saidi, M.; Douvinet, J.; Fehri, N.; Nasrallah, W.; Menad, W.; Mellas, S. Urbanization and land use as a driver of flood risk. In *The Mediterranean Region under Climate Change*; IRD Éditions: Marseille, France, 2016; Sub-chapter 3.4.1; pp. 563–575.
9. Aide, T.; Szönyi, M.; Saidi, A.D. *Morocco Floods of 2014: What We Can Learn from Guelmim and Sidi Ifni*; Zurich Insurance Group Ltd.: Zurichh, Switzerland, 2015.
10. Saidi, M.E.M.; Saouabe, T.; El Alaoui El Fels, A.; El Khalki, E.M.; Hadri, A. Hydro-meteorological characteristics and occurrence probability of extreme flood events in Moroccan High Atlas. *J. Water Clim. Chang.* **2020**. [CrossRef]
11. Gilles, D. Aménager, canaliser, encadrer juridiquement les rivières du Québec: Le poids de l'histoire? *Les Cahiers de Droit* **2011**, *51*, 923–945. [CrossRef]
12. Richter, B.D.; Thomas, G.A. Restoring environmental flows by modifying dam operations. *Ecol. Soc.* **2007**, *12*. [CrossRef]
13. Halwatura, D.; Najim, M.M.M. Application of the HEC-HMS model for runoff simulation in a tropical catchment. *Environ. Model. Softw.* **2013**, *46*, 155–162. [CrossRef]
14. Butts, M.B.; Payne, J.T.; Kristensen, M.; Madsen, H. An evaluation of the impact of model structure on hydrological modelling uncertainty for streamflow simulation. *J. Hydrol.* **2004**, *298*, 242–266. [CrossRef]
15. Gupta, H.V.; Kling, H.; Yilmaz, K.K.; Martinez, G.F. Decomposition of the mean squared error and NSE performance criteria: Implications for improving hydrological modelling. *J. Hydrol.* **2009**, *377*, 80–91. [CrossRef]
16. Ludwig, R.; May, I.; Turcotte, R.; Vescovi, L.; Braun, M.; Cyr, J.-F.; Fortin, L.-G.; Chaumont, D.; Biner, S.; Chartier, I.; et al. The role of hydrological model complexity and uncertainty in climate change impact assessment. *Adv. Geosci.* **2009**, *21*, 63–71. [CrossRef]

17. Wagener, T.; McIntyre, N. Identification of rainfall-runoff models for operational applications. *Hydrol. Sci. J.* **2005**, *50*, 735–751. [CrossRef]
18. El Khalki, E.M.; Tramblay, Y.; Saidi, M.E.M.; Bouvier, C.; Hanich, L.; Benrhanem, M.; Alaouri, M. Comparison of modeling approaches for flood forecasting in the High Atlas Mountains of Morocco. *Arab. J. Geosci.* **2018**, *11*, 410. [CrossRef]
19. Berthet, L.; Andréassian, V.; Perrin, C.; Javelle, P. *How Crucial Is It to Account for the Antecedent Moisture Conditions in Flood Forecasting? Comparison of Event-Based and Continuous Approaches on 178 Catchments*; European Geosciences Union: Munich, Germany, 2009; Volume 13, pp. 819–831.
20. Adler, R.F.; Huffman, G.J.; Chang, A.; Ferraro, R.; Xie, P.-P.; Janowiak, J.; Rudolf, B.; Schneider, U.; Curtis, S.; Bolvin, D.; et al. The Version-2 Global Precipitation Climatology Project (GPCP) Monthly Precipitation Analysis (1979–Present). *J. Hydrometeorol.* **2003**, *4*, 1147–1167. [CrossRef]
21. Hong, Y.; Hsu, K.L.; Sorooshian, S.; Gao, X. Precipitation estimation from remotely sensed imagery using an artificial neural network cloud classification system. *J. Appl. Meteorol.* **2004**, *43*, 1834–1852. [CrossRef]
22. Tramblay, Y.; Thiemig, V.; Dezetter, A.; Hanich, L. Evaluation of satellite-based rainfall products for hydrological modelling in Morocco. *Hydrol. Sci. J.* **2016**, *61*, 2509–2519. [CrossRef]
23. Kidd, C.; Kniveton, D.R.; Todd, M.C.; Bellerby, T.J. Satellite rainfall estimation using combined passive microwave and infrared algorithms. *J. Hydrometeorol.* **2003**, *4*, 1088–1104. [CrossRef]
24. Sorooshian, S.; Hsu, K.-L.; Gao, X.; Gupta, H.V.; Imam, B.; Braithwaite, D.; Sorooshian, S.; Hsu, K.-L.; Gao, X.; Gupta, H.V.; et al. Evaluation of PERSIANN System Satellite-Based Estimates of Tropical Rainfall. *Bull. Am. Meteorol. Soc.* **2000**, *81*, 2035–2046. [CrossRef]
25. Joyce, R.J.; Janowiak, J.E.; Arkin, P.A.; Xie, P. CMORPH: A Method that Produces Global Precipitation Estimates from Passive Microwave and Infrared Data at High Spatial and Temporal Resolution. *J. Hydrometeorol.* **2004**, *5*, 487–503. [CrossRef]
26. Huffman, G.J.; Bolvin, D.T.; Nelkin, E.J.; Wolff, D.B.; Adler, R.F.; Gu, G.; Hong, Y.; Bowman, K.P.; Stocker, E.F. The TRMM Multisatellite Precipitation Analysis (TMPA): Quasi-Global, Multiyear, Combined-Sensor Precipitation Estimates at Fine Scales. *J. Hydrometeorol.* **2007**, *8*, 38–55. [CrossRef]
27. Hou, A.Y.; Kakar, R.K.; Neeck, S.; Azarbarzin, A.A.; Kummerow, C.D.; Kojima, M.; Oki, R.; Nakamura, K.; Iguchi, T. The global precipitation measurement mission. *Bull. Am. Meteorol. Soc.* **2014**, *95*, 701–722. [CrossRef]
28. Hughes, D.A. Comparison of satellite rainfall data with observations from gauging station networks. *J. Hydrol.* **2006**, *327*, 399–410. [CrossRef]
29. Ward, E.; Buytaert, W.; Peaver, L.; Wheater, H. Evaluation of precipitation products over complex mountainous terrain: A water resources perspective. *Adv. Water Resour.* **2011**, *34*, 1222–1231. [CrossRef]
30. Bastola, S.; François, D. Temporal extension of meteorological records for hydrological modelling of Lake Chad Basin (Africa) using satellite rainfall data and reanalysis datasets. *Meteorol. Appl.* **2012**, *19*, 54–70. [CrossRef]
31. Liu, Y.Y.; Dorigo, W.A.; Parinussa, R.M.; De Jeu, R.A.M.; Wagner, W.; McCabe, M.F.; Evans, J.P.; van Dijk, A.I.J.M. Trend-preserving blending of passive and active microwave soil moisture retrievals. *Remote Sens. Environ.* **2012**, *123*, 280–297. [CrossRef]
32. Thiemig, V.; Rojas, R.; Zambrano-Bigiarini, M.; Levizzani, V.; De Roo, A. Validation of Satellite-Based Precipitation Products over Sparsely Gauged African River Basins. *J. Hydrometeorol.* **2012**, *13*, 1760–1783. [CrossRef]
33. Gosset, M.; Viarre, J.; Quantin, G.; Alcoba, M. Evaluation of several rainfall products used for hydrological applications over West Africa using two high-resolution gauge networks. *Q. J. R. Meteorol. Soc.* **2013**, *139*, 923–940. [CrossRef]
34. Xue, X.; Hong, Y.; Limaye, A.S.; Gourley, J.J.; Huffman, G.J.; Khan, S.I.; Dorji, C.; Chen, S. Statistical and hydrological evaluation of TRMM-based Multi-satellite Precipitation Analysis over the Wangchu Basin of Bhutan: Are the latest satellite precipitation products 3B42V7 ready for use in ungauged basins? *J. Hydrol.* **2013**, *499*, 91–99. [CrossRef]
35. Panegrossi, G.; Casella, D.; Dietrich, S.; Marra, A.C.; Sano, P.; Mugnai, A.; Baldini, L.; Roberto, N.; Adirosi, E.; Cremonini, R.; et al. Use of the GPM Constellation for Monitoring Heavy Precipitation Events over the Mediterranean Region. *IEEE J. Sel. Top. Appl. Earth Obs. Remote Sens.* **2016**, *9*, 2733–2753. [CrossRef]

36. Chiaravalloti, F.; Brocca, L.; Procopio, A.; Massari, C.; Gabriele, S. Assessment of GPM and SM2RAIN-ASCAT rainfall products over complex terrain in southern Italy. *Atmos. Res.* **2018**, *206*, 64–74. [CrossRef]
37. Chen, F.; Li, X. Evaluation of IMERG and TRMM 3B43 monthly precipitation products over mainland China. *Remote Sens.* **2016**, *8*, 472. [CrossRef]
38. Lu, X.; Wei, M.; Tang, G.; Zhang, Y. Evaluation and correction of the TRMM 3B43V7 and GPM 3IMERGM satellite precipitation products by use of ground-based data over Xinjiang, China. *Environ. Earth Sci.* **2018**, *77*. [CrossRef]
39. Milewski, A.; Elkadiri, R.; Durham, M. Assessment and Comparison of TMPA Satellite Precipitation Products in Varying Climatic and Topographic Regimes in Morocco. *Remote Sens.* **2015**, *7*, 5697–5717. [CrossRef]
40. Ouatiki, H.; Boudhar, A.; Tramblay, Y.; Jarlan, L.; Benabdelouhab, T.; Hanich, L.; El Meslouhi, M.R.; Chehbouni, A. Evaluation of TRMM 3B42 V7 rainfall product over the Oum Er Rbia watershed in Morocco. *Climate* **2017**, *5*, 1. [CrossRef]
41. Siccardi, F. Rainstorm Hazards and Related Disasters in the North-West Mediterranean Region. *Remote Sens. Rev.* **1996**, *14*, 5–21. [CrossRef]
42. Moret, L. *Carte Géologique Provisoire de l'Atlas de Marrakech [Document Cartographique]*; Ministry of Energy and Mines: Rabat, Morocco, 1930.
43. Proust, F. Tectonique de socle par failles inverses, en liaison avec d'anciennes failles normales dans le Haut Atlas (Maroc). *C.R. Somm. Soc. géol. Fr.* **1962**, *1*, 9–11.
44. Petit, J.P. La Zone de Décrochement du Tizi n'Test (Maroc) et Son Fonctionnement Depuis le Carbonifère. Ph.D. Thesis, University of Montpellier, Montpellier, France, 1976.
45. Dorigo, W.; Wagner, W.; Albergel, C.; Albrecht, F.; Balsamo, G.; Brocca, L.; Chung, D.; Ertl, M.; Forkel, M.; Gruber, A.; et al. ESA CCI Soil Moisture for improved Earth system understanding: State-of-the art and future directions. *Remote Sens. Environ.* **2017**, *203*, 185–215. [CrossRef]
46. Gruber Leuven, A.K.; Gruber, A.; Arnoud Dorigo, W.; Crow, W.; Wagner, W.; Member, S. Triple Collocation-Based Merging of Satellite Soil Moisture Retrievals Integrating microwave and thermal remote sensing for continuous dual source surface energy balance modeling View project AirMOSS View project Triple Collocation-Based Merging of Satellite Soil Moisture Retrievals. *IEEE Trans. Geosci. Remote Sens.* **2017**, *55*. [CrossRef]
47. Dorigo, W.A.; Gruber, A.; de Jeu, R.A.M.; Wagner, W.; Stacke, T.; Loew, A.; Albergel, C.; Brocca, L.; Chung, D.; Parinussa, R.M.; et al. Evaluation of the ESA CCI soil moisture product using ground-based observations. *Remote Sens. Environ.* **2015**, *162*, 380–395. [CrossRef]
48. El Khalki, E.M.; Tramblay, Y.; Amengual, A.; Homar, V.; Romero, R.; Saidi, M.E.M.; Alaouri, M. Validation of the AROME, ALADIN and WRF Meteorological Models for Flood Forecasting in Morocco. *Water* **2020**, *12*, 437. [CrossRef]
49. El Khalki, E.M.M.; Tramblay, Y.; Massari, C.; Brocca, L.; Simonneaux, V.; Gascoin, S.; Saidi, M.E.M. Challenges in flood modelling over data scarce regions: How to exploit globally available soil moisture products to estimate antecedent soil wetness conditions in Morocco. *Nat. Hazards Earth Syst. Sci. Discuss.* **2020**. [CrossRef]
50. US Army Corps of Engineers Hydrologic Engineering Center. *Technical Reference Manual Version 3.5*; US Army Corps of Engineers Hydrologic Engineering Center: Davis, CA, USA, 2010.
51. Tramblay, Y.; Bouaicha, R.; Brocca, L.; Dorigo, W.; Bouvier, C.; Camici, S.; Servat, E. Antecedent wetness conditions for flood modelling in Northern Morocco Hydrology and Earth System Sciences Discussions Estimation of antecedent wetness conditions for flood modelling in Northern Morocco Antecedent wetness conditions for flood modelling in Northern Morocco. *Hydrol. Earth Syst. Sci. Discuss.* **2012**, *9*, 9361–9390. [CrossRef]
52. Nash, J.E.; Sutcliffe, J.V. River flow forecasting through conceptual models Part I—A discussion of principles. *J. Hydrol.* **1970**, *10*, 282–290. [CrossRef]
53. Huang, M.; Gallichand, J.; Dong, C.; Wang, Z.; Shao, M. Use of soil moisture data and curve number method for estimating runoff in the Loess Plateau of China. *Hydrol. Process.* **2007**, *21*, 1471–1481. [CrossRef]
54. Brocca, L.; Melone, F.; Moramarco, T.; Singh, V.P. Assimilation of observed soil moisture data in storm rainfall-runoff modeling. *J. Hydrol. Eng.* **2009**, *14*, 153–165. [CrossRef]
55. Tramblay, Y.; Bouvier, C.; Martin, C.; Didon-Lescot, J.F.; Todorovik, D.; Domergue, J.M. Assessment of initial soil moisture conditions for event-based rainfall-runoff modelling. *J. Hydrol.* **2010**, *387*, 176–187. [CrossRef]

56. Brocca, L.; Melone, F.; Moramarco, T.; Wagner, W.; Hasenauer, S. ASCAT soil wetness index validation through in situ and modeled soil moisture data in central Italy. *Remote Sens. Environ.* **2010**, *114*, 2745–2755. [CrossRef]
57. Caracciolo, D.; Francipane, A.; Viola, F.; Noto, L.V.; Deidda, R. Performances of GPM satellite precipitation over the two major Mediterranean islands. *Atmos. Res.* **2018**, *213*, 309–322. [CrossRef]
58. Zubieta, R.; Getirana, A.; Espinoza, J.C.; Lavado-Casimiro, W.; Aragon, L. Hydrological modeling of the Peruvian-Ecuadorian Amazon basin using GPM-IMERG satellite-based precipitation dataset. *Hydrol. Earth Syst. Sci.* **2016**, 3543–3555. [CrossRef] [PubMed]
59. Hosseini-Moghari, S.M.; Tang, Q. Validation of gpm imerg v05 and v06 precipitation products over iran. *J. Hydrometeorol.* **2020**, *21*, 1011–1037. [CrossRef]
60. Navarro, A.; García-ortega, E.; Merino, A.; Sánchez, L.; Tapiador, F.J. Orographic biases in IMERG precipitation estimates in the Ebro River basin (Spain): The effects of rain gauge density and altitude. *Atmos. Res.* **2020**, 105068. [CrossRef]
61. Tapiador, F.J.; Navarro, A.; García-Ortega, E.; Merino, A.; Sánchez, J.L.; Marcos, C.; Kummerow, C. The contribution of rain gauges in the calibration of the IMERG product: Results from the first validation over Spain. *J. Hydrometeorol.* **2020**, *21*, 161–182. [CrossRef]
62. Fang, J.; Yang, W.; Luan, Y.; Du, J.; Lin, A.; Zhao, L. Evaluation of the TRMM 3B42 and GPM IMERG products for extreme precipitation analysis over China. *Atmos. Res.* **2019**, *223*, 24–38. [CrossRef]
63. Gilewski, P.; Nawalany, M. Inter-comparison of Rain-Gauge, Radar, and Satellite (IMERG GPM) precipitation estimates performance for rainfall-runoff modeling in a mountainous catchment in Poland. *Water* **2018**, *10*, 1665. [CrossRef]
64. Massari, C.; Brocca, L.; Barbetta, S.; Papathanasiou, C.; Mimikou, M.; Moramarco, T. Using globally available soil moisture indicators for flood modelling in Mediterranean catchments. *Hydrol. Earth Syst. Sci* **2014**, *18*, 839–853. [CrossRef]
65. Norbiato, D.; Borga, M.; Degli Esposti, S.; Gaume, E.; Anquetin, S. Flash flood warning based on rainfall thresholds and soil moisture conditions: An assessment for gauged and ungauged basins. *J. Hydrol.* **2008**, *362*, 274–290. [CrossRef]
66. Sharifi, E.; Steinacker, R.; Saghafian, B. Assessment of GPM-IMERG and other precipitation products against gauge data under different topographic and climatic conditions in Iran: Preliminary results. *Remote Sens.* **2016**, *8*, 135. [CrossRef]